Surface Chemistry

DOI: 10.1002/ange.201304688

# Light-Activated Electroactive Molecule-Based Memory Microcells Confined on a Silicon Surface**

*Bruno Fabre,* Yan Li, Luc Scheres, Sidharam P. Pujari, and Han Zuilhof**

Among the existing charge-storage devices of modern computers, the dynamic random access memory (DRAM) provides the most interesting opportunity of integrating redox-active molecular components.[1] The capacitance density of today's DRAM storage cell is on the order of 50–100 $fF\,\mu m^{-2}$ (5–10 $\mu F\,cm^{-2}$) with a benchmark cell size below the square-micrometer range. In this context, ferrocene (Fc) and metal-complexed porphyrins have been explored as the most promising memory elements, because they show, both in solution and confined on surfaces, one to several perfectly reversible and stable one-electron redox reactions within an attractive potential window, that is, 0.0 to 1.0 V vs. a saturated calomel electrode (SCE). Therefore, the functionalization of technologically relevant conducting surfaces, such as oxide-free, hydrogen-terminated silicon (H-Si), with high-quality Fc-terminated[2–8] and metal-complexed porphyrin-terminated[9–12] monolayers has been demonstrated to be a powerful bottom-up approach for the fabrication of electrically addressable charge-storage devices with low-power consumption. Compared with metalloporphyrins, Fc is a much smaller molecule (average diameter of tetraphenylporphyrin and Fc are about 18 and 6.6 Å, respectively), and consequently is immobilized on silicon with a higher surface coverage, which gives rise to higher charge densities. Indeed, the surface coverages reached for high-quality ferrocenyl monolayers are in the range of $(2.0–5.0)\times10^{-10}$ $mol\,cm^{-2}$. This does not only allow for an extremely fast electron communication between the electroactive groups,[5] but also yields charge densities in the range of 20–50 $\mu C\,cm^{-2}$.[2] These values are thus much higher than those measured for $Si/SiO_2$ capacitors currently used in DRAM memories (5–10 $\mu C\,cm^{-2}$).

Herein, we demonstrate that tailor-made micrometer-sized patterns of such redox-active monolayers can behave as light-activated molecular memory cells with unprecedented capacitance performances, and can be constructed so as to yield an efficient AND logical gate. To reach this challenging prospect, we chose n-type silicon substrates as immobilization platforms. For oxidation processes, n-type silicon behaves as an insulator in the dark, and as a quasi-conductor upon illumination,[13] providing a unique way to communicate efficiently with the charge-storage centers when the light is turned on. Since our molecular switches are based on two states (ON and OFF states), they also offer great potential for the development of binary logic gates using the electrical voltage as an input function.

The functional surfaces were prepared by microcontact printing (μCP), in which a polydimethylsiloxane (PDMS) stamp[14] was inked by an amino-substituted Fc[6] onto a preformed, reactive, acid fluoride-terminated alkenyl monolayer[15] covalently bound to n-type H-Si(111) (Figure 1, see also the Supporting Information).[4] Compared with Si–C–C-linked monolayers prepared from 1-alkenes,[16–18] 1-alkyne-derived monolayers are usually both more ordered and displaying a higher surface coverage.[19–21] The unstamped regions were then backfilled with butylamine to produce nonelectroactive, butylamide-terminated chains around the patterns. This patterning method resulted in $5\times5\,\mu m^2$ Fc-functionalized squares separated by 5 μm of butylamide-terminated areas, yielding $10^6$ ferrocenyl microstructures per square centimeter of the electrode. The pattern is evident from AFM phase imaging, which displays the large differences in the chemical composition between the two regions, and SEM images (Figures S6 and S8 in the Supporting Information). In addition, also spot analysis by scanning auger electron spectroscopy (SAES) displays the differences in elemental composition of the spots and the background, and so confirms the chemical nature of the Fc monolayer spots (Figure S7 and Table S2 in the Supporting Information).

The different derivatized surfaces were further characterized by ellipsometry, contact angle measurements and X-ray photoelectron spectroscopy (XPS). All these techniques confirmed the formation of densely packed monolayers at each grafting step with both the expected molecular composition and thickness, and without detectable oxidation of underlying silicon (see the Supporting Information).

Voltammetric analysis of the micropatterned Fc-modified surface in the dark shows the absence of a significant oxidation current response. Upon illumination (white light generated using a 50 W tungsten halogen lamp), a well-

[*] Prof. Dr. B. Fabre
Institut des Sciences Chimiques de Rennes
UMR 6226 CNRS/Université de Rennes 1
Matière Condensée et Systèmes Electroactifs (MaCSE)
Campus de Beaulieu, 35042 Rennes Cedex (France)
E-mail: fabre@univ-rennes1.fr
Dr. Y. Li, Dr. L. Scheres, Dr. S. P. Pujari, Prof. Dr. H. Zuilhof
Laboratory of Organic Chemistry, Wageningen University
Dreijenplein 8, 6703 HB Wageningen (The Netherlands)
E-mail: han.zuilhof@wur.nl
Dr. L. Scheres
Surfix B.V.
Dreijenplein 8, 6703 HB Wageningen (The Netherlands)
Prof. Dr. H. Zuilhof
Department of Chemical and Materials Engineering
King Abdulaziz University, Jeddah (Saudi Arabia)

[**] This work was partially supported by the CNRS, Agence Nationale de la Recherche ANR (project number 09-BLAN-0109).

Supporting information for this article is available on the WWW under http://dx.doi.org/10.1002/anie.201304688.

  

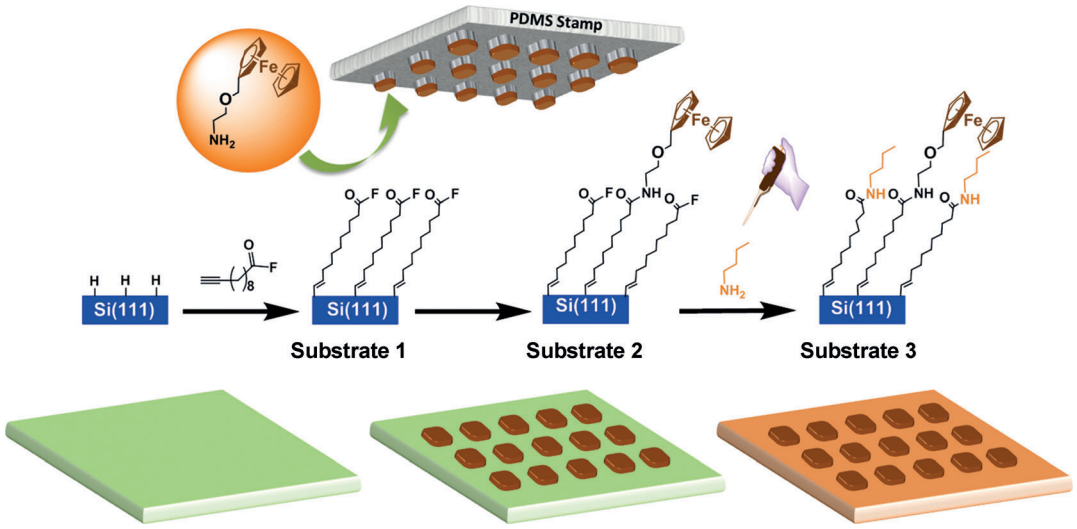


***Figure 1.*** Preparation of ultrahigh-capacity ferrocene-based memory microcells confined on a n-type Si(111) surface.

defined reversible wave corresponding to the oxidation of Fc to ferrocenium ($Fc^+$) appears at a formal potential $E^{\circ\prime} = 0.07 \pm 0.01$ V vs. SCE (Figure 2A). As predicted for surface-confined reversible redox species, the peak currents are proportional to the potential scan rate $\nu$. Moreover, we note, in line with other reports,[2,4,22] that the $E^{\circ\prime}$ of Fc bound to n-type Si under illumination is about 300–400 mV lower than that observed for Fc bound to p-type Si,[2] as a result of activation of the redox process by photogenerated electron–hole pairs.[23] The total surface density of attached Fc moieties was estimated by integration of cyclic voltammetry peak to be $(1.2 \pm 0.1) \times 10^{-10}$ mol per square centimeter of electrode. Considering the fractional coverage of the electroactive sites (namely a quarter of the total area), this value corresponds to $(4.8 \pm 0.4) \times 10^{-10}$ mol per square centimeter of the electroactive patterns. This is perfectly in line with the ball-like shape of the Fc molecules with a diameter of 6.6 Å and indicative for a high-quality, densely packed Fc monolayer inside the patterns.

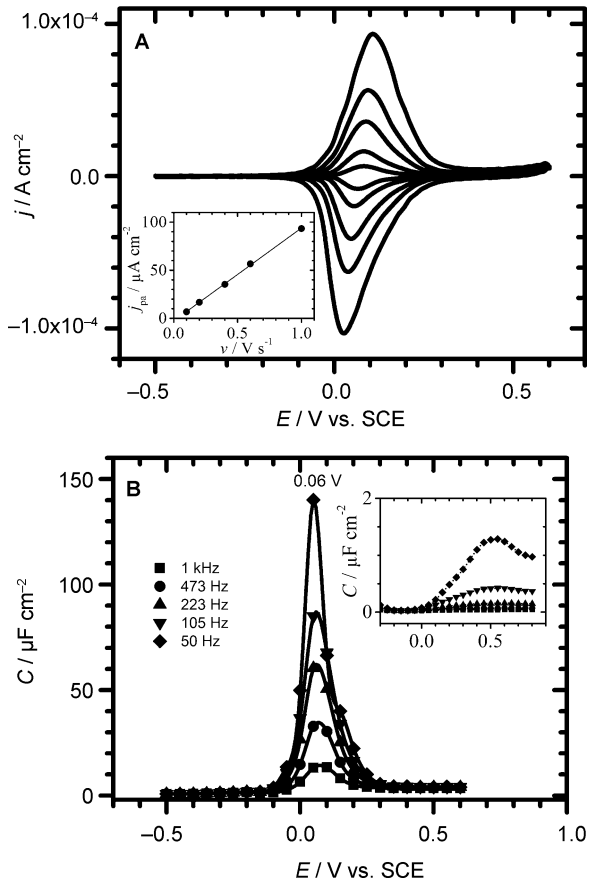


***Figure 2.*** A) Cyclic voltammograms under illumination (white light generated using a 50 W tungsten halogen lamp) of the micropatterned Fc-modified surface at 0.1, 0.2, 0.4, 0.6, and 1 $Vs^{-1}$. The inset shows the corresponding $j_{pa}$–$\nu$ plot. B) Corresponding capacitance–potential curves measured at different frequencies under illumination and as shown in the inset in the dark. Electrolyte: $CH_3CN + 0.1$ M $Bu_4NClO_4$.

By taking advantage of the fact that the communication with the charge-storage centers can be turned on with light, the charge-storage characteristics of our micrometer-sized electrolyte–molecule–silicon (EMS) capacitor structures have been examined using electrochemical impedance spectroscopy (EIS) with and without light. In the dark, the measured frequency-dependent capacitance values are very small and do not exceed 1 $\mu F\,cm^{-2}$. In contrast, the capacitance curves under illumination are characterized by a much more intense capacitance peak at a potential relatively close to the $E^{\circ\prime}$ of bound Fc, the amplitude of which increases with decreasing the measurement frequency (Figure 2B).[24] For example, a maximum capacitance of 120–140 $\mu F\,cm^{-2}$ was measured at 50 Hz, which demonstrates the high photoinduced charge-storage capacity of our hybrid device. These capacitance peaks were not observed for nonelectroactive organic monolayers, and therefore were clearly attributed to the charging/discharging currents associated with the oxidation/reduction of bound $Fc/Fc^+$.[25,26]

Figure 3 shows the time profiles of capacitance at different applied potentials with (ON state) and without light (OFF state). The capacitance of the electrode at 50 Hz can be switched from a few $10^{-1}$ $\mu F\,cm^{-2}$ in the dark to approx-

  

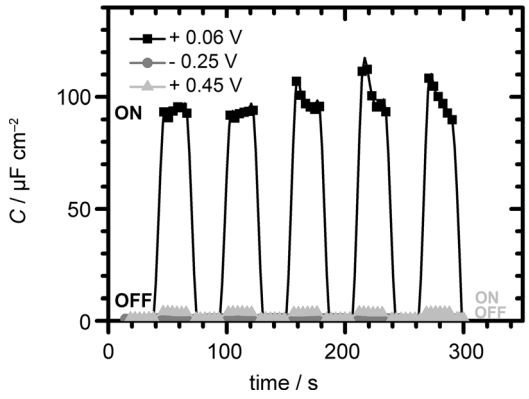


***Figure 3.*** Capacitance–time profiles at 50 Hz of the micropatterned Fc-modified surface measured at different applied potentials during several dark (OFF state)/illumination (ON state) switching cycles. Illumination with white light was generated using a 50 W tungsten halogen lamp.

imately 100 µF cm$^{-2}$ under illumination when the applied potential is 0.06 V. Consistent with the potential-dependent response, the capacitance switching was much lower for potentials located before and after the capacitance peak. The high capacitance state was retained as long as the voltage was applied, and remained constant over numerous ON/OFF switching cycles. Only a 10% decrease in the maximum photocapacitance was observed after $10^3$ ON/OFF switching cycles (Figure 4). We have also checked that the electroactive centers were responsible for this remarkable observed photoactivity. Under similar illumination conditions, the photocapacitance of silicon uniformly modified with nonelectroactive butylamide-terminated monolayer remains negligible, with less than 10% of the maximum capacitance reached by the ferrocene-functionalized device (Figure 4 A).

The characteristics of this stimuli-responsive device are of great scientific interest for data-processing applications, such as redox-based Boolean logic gates.[27–31] In fact, the switching of the capacitance upon light irradiation that is observed only at a certain electrical potential can be applied for constructing a two-input AND logic gate. The two inputs can be defined as the illumination level and the applied electrical potential, whereas the capacitance measured at 50 Hz can be considered as the output signal, with output = "0" when the capacitance is below 2 µF cm$^{-2}$ and output = "1" when the capacitance is higher than the threshold value of 80 µF cm$^{-2}$. The system is in state "1" only if both the interface is illuminated and the electrical potential is fixed at about 0.06 V (i.e. close to the formal potential of the Fc/Fc$^+$ couple). All the other combinations yield an output signal "0" with an interesting magnitude difference of 50 times at least between the output signals "0" and "1". The truth table shown in Figure 5 summarizes the operation realized by such a redox-active molecular logic gate. This is, as far as we know, the first all solid-state molecular AND gate: it is entirely optically and electrically addressable and does not require the addition of chemical inputs in solution to function. As such, it is really different from that based on other outstanding redox-active, functionalized surfaces, such as reported by van der Boom and co-workers.[27,28]

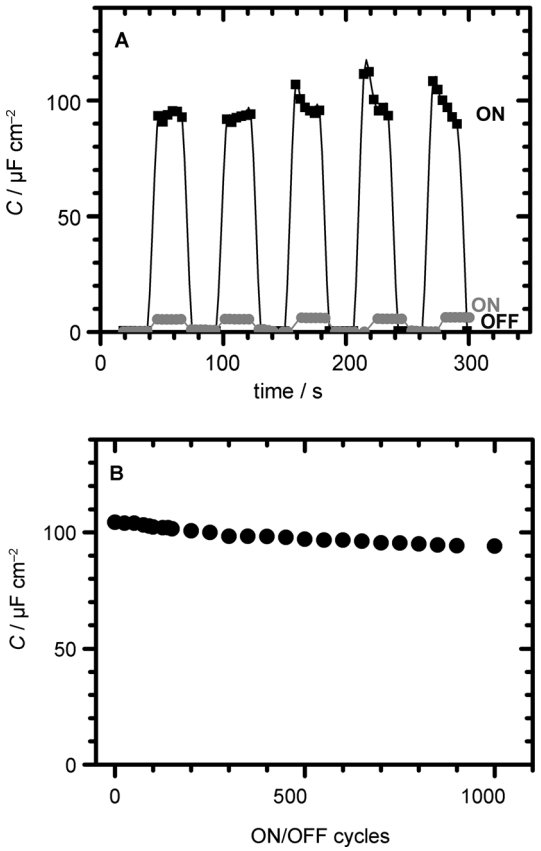


***Figure 4.*** A) Comparative capacitance–time profiles at 50 Hz of the micropatterned Fc-modified surface (black) and the non-electroactive single-component butylamide-terminated monolayer-modified surface (gray) measured at 0.10 ± 0.05 V during several dark (OFF)/illumination (ON) switching cycles. B) Stability of the photocapacitance measured at 50 Hz for an applied potential of 0.06 V vs. SCE as a function of the number of ON/OFF cycles. Illumination with white light was generated using a 50 W tungsten halogen lamp.

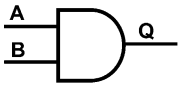


| Input A | Input B | Output Q |
|---|---|---|
| 0 | 0 | 0 (0.6 ± 0.2) |
| 0 | 1 | 0 (0.2 ± 0.1) |
| 1 | 0 | 0 (1.1 ± 0.1) |
| 1 | 1 | 1 (100 ± 10) |

***Figure 5.*** Truth table for AND logic gate based on Fc-functionalized silicon surfaces using the illumination level ("0" and "1" states for dark and illuminated conditions) and the applied electrical potential ("0" and "1" states for −0.25 and + 0.06 V vs. SCE) as the "A" and "B" inputs, respectively. The output is the capacitance response measured at a frequency of 50 Hz (in µF cm$^{-2}$).

In conclusion, we have fabricated a molecular photoswitch and an all-solid AND logic gate device using redox-active ferrocene micropatterns confined on silicon surfaces. This system operates at a particularly attractive potential of about 0.1 V vs. SCE and yields capacitance values of about 100 µF cm$^{-2}$ with ON/OFF ratios reaching $10^3$. Such performances, which can be ascribed to the judicious combination between a photoswitchable conducting/insulating substrate

and high-quality redox-active assemblies, demonstrate the potential of these interfaces for molecular memory devices. Another stimulating prospect of this research is that such interfaces are also excellent platforms to produce other molecular logic functions. By using silicon surfaces micropatterned with two redox centers electrochemically oxidizable or reducible at two well-separated potentials (instead of non-electroactive butylamide-terminated regions as in the present study), it should be possible to fabricate a series of all solid-state multi-input redox-based logic circuits. Toward this challenging goal, silicon surfaces micropatterned with two different metallocenes or differently substituted Fc-derivatives are currently under preparation in our groups.

Received: May 30, 2013
Published online: September 23, 2013

**Keywords:** charge transfer · ferrocene · monolayers · silicon · surface chemistry

[1] International Technology Roadmap for Semiconductors (ITRS): process, integration, devices, and structures. Semiconductor Industry Association, San Jose, California, **2011**. http://www.itrs.net/reports.html.
[2] B. Fabre, *Acc. Chem. Res.* **2010**, *43*, 1509 – 1518.
[3] S. P. Cummings, J. Savchenko, T. Ren, *Coord. Chem. Rev.* **2011**, *255*, 1587 – 1602.
[4] D. Zigah, C. Herrier, L. Scheres, M. Giesbers, B. Fabre, P. Hapiot, H. Zuilhof, *Angew. Chem.* **2010**, *122*, 3225 – 3228; *Angew. Chem. Int. Ed.* **2010**, *49*, 3157 – 3160.
[5] F. Hauquier, J. Ghilane, B. Fabre, P. Hapiot, *J. Am. Chem. Soc.* **2008**, *130*, 2748 – 2749.
[6] B. Fabre, F. Hauquier, *J. Phys. Chem. B* **2006**, *110*, 6848 – 6855.
[7] F. Decker, F. Cattaruzza, C. Coluzza, A. Flamini, A. G. Marrani, R. Zanoni, E. A. Dalchiele, *J. Phys. Chem. B* **2006**, *110*, 7374 – 7379.
[8] N. Tajimi, H. Sano, K. Murase, K.-H. Lee, H. Sugimura, *Langmuir* **2007**, *23*, 3193 – 3198.
[9] J. S. Lindsey, D. F. Bocian, *Acc. Chem. Res.* **2011**, *44*, 638 – 650.
[10] K. M. Roth, A. A. Yasseri, Z. Liu, R. B. Dabke, V. Malinovskii, K.-H. Schweikart, L. Yu, H. Tiznado, F. Zaera, J. S. Lindsey, W. G. Kuhr, D. F. Bocian, *J. Am. Chem. Soc.* **2003**, *125*, 505 – 517.
[11] Z. Liu, A. A. Yasseri, J. S. Lindsey, D. F. Bocian, *Science* **2003**, *302*, 1543 – 1545.
[12] K. Huang, F. Duclairoir, T. Pro, J. Buckley, G. Marchand, E. Martinez, J.-C. Marchon, B. De Salvo, G. Delapierre, F. Vinet, *ChemPhysChem* **2009**, *10*, 963 – 971.
[13] X. G. Zhang in *Electrochemistry of Silicon and its Oxide*, Kluwer Academic/Plenum Publishers, New York, **2001**.
[14] B. J. Ravoo, *J. Mater. Chem.* **2009**, *19*, 8902 – 8906, and references therein.
[15] L. Scheres, J. ter Maat, M. Giesbers, H. Zuilhof, *Small* **2010**, *6*, 642 – 650.
[16] J. M. Buriak, *Chem. Rev.* **2002**, *102*, 1271 – 1308.
[17] S. Ciampi, J. B. Harper, J. J. Gooding, *Chem. Soc. Rev.* **2010**, *39*, 2158 – 2183.
[18] M. R. Linford, P. Fenter, P. M. Eisenberger, C. E. D. Chidsey, *J. Am. Chem. Soc.* **1995**, *117*, 3145 – 3155.
[19] Y. Li, S. Calder, O. Yaffe, D. Cahen, H. Haick, L. Kronik, H. Zuilhof, *Langmuir* **2012**, *28*, 9920 – 9929.
[20] L. Scheres, B. Rijksen, M. Giesbers, H. Zuilhof, *Langmuir* **2011**, *27*, 972 – 980.
[21] A. Ng, S. Ciampi, M. James, J. B. Harper, J. J. Gooding, *Langmuir* **2009**, *25*, 13934 – 13941.
[22] S. Gowda, G. Mathur, V. Misra, *Appl. Phys. Lett.* **2007**, *90*, 142113.
[23] M. X. Tan, P. E. Laibinis, S. T. Nguyen, J. M. Kesselman, C. E. Stanton, N. S. Lewis in *Progress in Inorganic Chemistry, Vol. 41*, Wiley, New York, **1994**, pp. 21 – 144.
[24] In the dark, the total capacitance of the interface is dominated by the space charge of silicon but the measured values are negligible in comparison with those measured under illumination for which the contribution of charge-storage centers (i.e. Fc) becomes majority.
[25] J. Gonzalez, A. Molina, *J. Electroanal. Chem.* **2003**, *557*, 157 – 165.
[26] P. R. Bueno, F. Fabregat-Santiago, J. J. Davis, *Anal. Chem.* **2013**, *85*, 411 – 417.
[27] G. de Ruiter, M. E. van der Boom, *Acc. Chem. Res.* **2011**, *44*, 563 – 573.
[28] T. Gupta, M. E. van der Boom, *Angew. Chem.* **2008**, *120*, 5402 – 5406; *Angew. Chem. Int. Ed.* **2008**, *47*, 5322 – 5326.
[29] K. Szaciłowski, *Chem. Rev.* **2008**, *108*, 3481 – 3548.
[30] Y. Liu, A. Offenhäusser, D. Mayer, *Angew. Chem.* **2010**, *122*, 2649 – 2652; *Angew. Chem. Int. Ed.* **2010**, *49*, 2595 – 2598.
[31] C. P. Collier, E. W. Wong, M. Belohradsky, F. M. Raymo, J. F. Stoddart, P. J. Kuekes, R. S. Williams, J. R. Heath, *Science* **1999**, *285*, 391 – 394.

  